Experimental and theoretical investigation of the Stark effect for manipulating cold molecules: Application to nitric oxide

Bryan J. Bichsel, Michael A. Morrison,* Neil Shafer-Ray, and E. R. I. Abraham
Department of Physics and Astronomy, The University of Oklahoma, 440 West Brooks Street, Norman, Oklahoma 73019-0225, USA
(Received 9 June 2006; published 22 February 2007)

As part of an ongoing investigation of cold-molecule collisions involving nitric oxide (NO), we here theoretically assess the first- and second-order perturbation-theory approximations to the Stark shifts; such approximations have been used almost exclusively in previous published research on NO in external electric fields. We perform this assessment by comparison to Stark shifts from the corresponding nonperturbative two-state model, considering field strengths from zero to values typical of current experimental studies of cold molecules. To facilitate the future use of this model, we give expressions for the Stark energies in a generic form that can trivially be applied to any molecules in the class under consideration. To provide insight into the validity of the two-state model, we also experimentally assess the two-state Stark shifts for NO.

DOI: 10.1103/PhysRevA.75.023410 PACS number(s): 33.55.Be, 33.80.Ps

I. INTRODUCTION

Laser cooling and trapping of atoms has produced a wealth of fundamental and applied physics because these techniques allow unprecedented control of the external degrees of freedom of the trapped particles (see, for example, Refs. [1–3]). A high point of this research was the production of Bose-Einstein condensation of dilute gases in traps formed by electromagnetic fields (see, for example, Refs. [4,5]). Because laser cooling lends itself most easily to the alkali metals, these experiments use conservative confining potentials with either static magnetic fields (the Zeeman effect) or laser fields (the ac Stark effect).

Currently researchers are developing new techniques for producing cold ($T \lesssim 1$ K) and ultracold ($T \lesssim 1$ mK) molecules [109]. The idea is to trap samples of cold paramagnetic or polar molecules using techniques similar to those that have successfully trapped alkali metal atoms [6,7]. The intense current interest in trapped cold molecules stems from several features of these systems. Cold molecules exhibit intriguing collision phenomena [8] and novel collision dynamics [9,10]. The chemistry may be controlled at the quantum level using static electromagnetic fields and modified through Feshbach resonances [11]. New molecular complexes can be created through photoassociation [12] or through field-linked states [13,14]. Cold molecules may serve as quantum computers [15]. Traps with nonzero field minima [16] may have sufficiently long trap lifetimes to enable measurement of the electric dipole moment of the electron using molecules [17–19].

Many molecules have permanent electric dipole moments, so their quantum states exhibit large dc Stark shifts. This property can be exploited to construct deep electrostatic confining potentials [7]. The present work was motivated in part by experimental programs at the University of Oklahoma [20] and elsewhere [21] to perform cold-molecule experiments on nitric oxide (NO) using electrostatic trapping techniques that involve the dc Stark effect at field strengths on the order of 100 kV/cm. Specifically, we are interested in NO in its ground ($^2\Pi$) state.

Prior theoretical [22,23] and experimental [24–29] research on the Stark effect in NO focused on *microwave spectroscopy*, where the applied electric fields are quite weak. This feature has two consequences that affect analysis of microwave spectra. First, for weak external fields, hyperfine effects must be incorporated into the theoretical analysis [26,30–35]. (Some microwave spectroscopy experiments on molecules other than NO require nonperturbative treatments similar to the one in this paper; see, for example, Ref. [36]). Second, for weak fields second-order perturbation theory—the quadratic Stark effect—accurately approximates the Stark shifts. Consequently, almost all prior literature on the Stark effect in NO makes heavy use of perturbative treatments. Neither of these consequences, however, necessarily pertains to the much stronger fields used in current Stark-effect-based techniques for cooling and trapping molecules.

To be sure, current computers often permit one to simply forego consideration of a perturbative treatment [110]. Cold-molecule physics, however, is one of several contexts in which the suitability of perturbation theory is an issue that may be of great importance. For example, the recent (2004) exhaustive analysis of the Stark slower by [37] uses perturbation-based Stark shifts to simplify subsequent mathematical analysis. Similarly, recent discussions of the feasibility of constructing a storage ring for polar molecules in strong-field seeking states [38,39] consider perturbative treatments of the Stark effect. Perturbation theory also plays a role in recent calculations related to the use of electric fields to align molecules [40,41]. Finally, work published since about 1980 on trajectory simulations of Stark hexapole guides for molecular beams have used either first-order [42–44] or second-order [45,46] perturbation theory, or a two-state model [47] similar to the one described in Sec. III. In recent literature on cold-molecule experiments that use the Stark effect, some use a perturbative theory (see, for example, Refs. [48–50]); many papers, however, do not contain information on how the Stark effect is treated (see, for example, Refs. [51–55]).

Although the present research concerns the Stark effect in NO, some of our results and conclusions pertain to other

*Electronic address: morrison@nhn.ou.edu

diatomic radicals with $^2\Pi$ ground electronic states in situations where the hyperfine Hamiltonian is negligible compared to other terms in the system Hamiltonian (including the Stark Hamiltonian), and the two states of interest are well-separated in energy from all other states. Even with these caveats, this study encompasses a number of important molecules, including LiO, OH, ClO, BeH, SH, PbF, YbF, and CH.

The present paper has two goals. The first goal is to investigate analytically and quantitatively the validity of perturbative treatments of the Stark effect *for NO at fields characteristic of current cold-molecule experiments*. The second goal is to shed light on the accuracy of the nonperturbative equations for the Stark shifts in NO. This goal we accomplish through comparison to experimental data.

Specifically, in Sec. III we adapt to the problem at hand—the Stark effect for NO (and similar molecules) at electric fields as large as 100 kV/cm—the two-state model of time-independent quantum mechanics [[56,57], p. 253] (see Sec. III A). We then obtain the approximate linear and quadratic Stark shifts of perturbation theory by truncating series expansions of the two-state shifts (Sec. III B). With this background, we compare these perturbative approximations to the two-state shifts in Sec. III C in order to quantify the errors introduced by perturbation theory for field strengths from 0 to 100 kV/cm. Within this range we have found errors in perturbative Stark shifts that are sufficiently large that the two-state model may be preferable.

To gain insight into the accuracy of the two-state model for cold-molecule experiments on NO, we compare two-state Stark shifts to data measured with the Stark guide described in Sec. IV. To facilitate use of the equations of the two-state model for radicals other than NO we present "generic forms" that can be applied trivially to any diatomic with a $^2\Pi$ ground electronic state (for detailed information about these molecules, see the compilation in Ref. [58]). While the venerable two-state model is not new to the quantum mechanics of Stark effect (see, for example, Refs. [36,47]), to our knowledge no previous publication quantitatively assesses the errors inherent in the linear and quadratic Stark shifts for field strengths characteristic of current cold- and ultracold molecule experiments (around 100 kV/cm).

To define a physical context for discussion of our results and to establish notation we begin in Sec. II by summarizing the relevant physics of zero-field states of NO. We also present contemporary values of spectroscopic and other data needed to calculate zero-field energies and Stark shifts for this molecule.

II. SUMMARY OF RELEVANT PROPERTIES OF NO

Molecules such as nitric oxide (NO) stand out among stable diatomic radicals in that they have an odd number of electrons and a $^2\Pi$ ground-state term. The latter corresponds to quantum numbers $S=1/2$ for the total electronic spin $\mathbf{S}$ and $\Lambda=\pm1$ for the projection of the total electronic orbital angular momentum on the internuclear axis $\mathbf{R}$. In its ground electronic state, NO is an open-shell, weakly polar radical whose dominant orbital configuration is

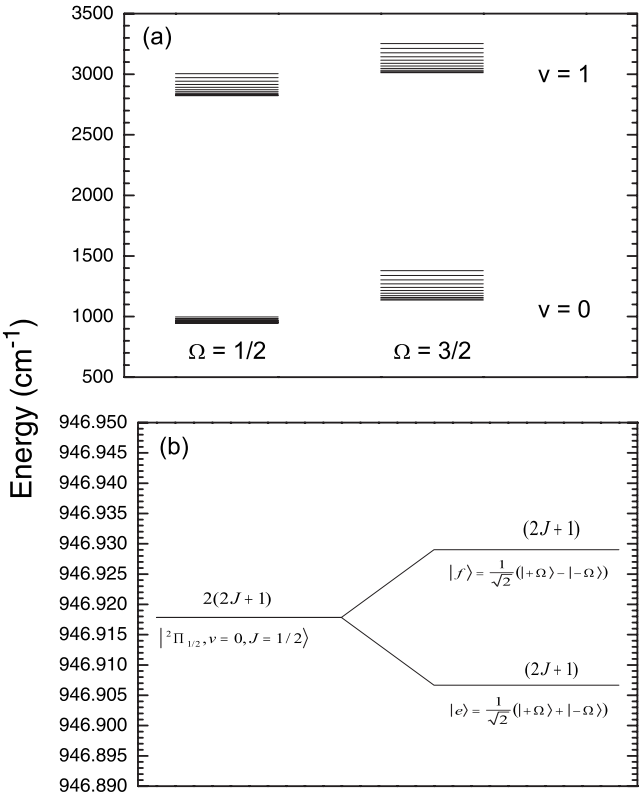

FIG. 1. Zero-field rovibronic energies of $^{14}N^{16}O$ relative to a zero of energy at the lowest spin-orbit level of the ground electronic term at the equilibrium internuclear separation R_e. (a) The 11 lowest rotational energies for the $v=0$ and $v=1$ vibrational manifolds of the $^2\Pi_{1/2}$ and $^2\Pi_{3/2}$ fine-structure levels. (b) The energies of the Λ-doublet levels for the $J=1/2$ states of the $v=0$ manifold of the $^2\Pi_{1/2}$ electronic state (on an expanded energy scale). Each level is labeled by its degree of degeneracy (above the line) and by the appropriate state designations (below the line); for the e and f states, see Eq. (A6b)

$1\sigma^2 2\sigma^2 3\sigma^2 4\sigma^2 5\sigma^2 1\pi^4 2\pi$. In this state, spin-orbit interactions yield a multiplet with $\Omega \equiv \Lambda+\Sigma=\pm1/2, \pm3/2$, where the quantum number Σ corresponds to the projection of $\mathbf{S}$ on $\mathbf{R}$. The spin-orbit multiplet is regular, the $^2\Pi_{3/2}$ level lying above the $^2\Pi_{1/2}$ level [59,60]. The quantitative effects of the spin-orbit interaction on the Born-Oppenheimer energies in the ground electronic state of NO are shown (to scale) in Fig. 1(a).

In NO, coupling of the electron spin to the internuclear axis is sufficiently strong that for low-lying rotational states, this molecule is accurately described by Hund's case (a) [25,31,61,62]. Strictly, this case is appropriate for values of the quantum number J, which corresponds to the total angular momentum excluding nuclear spin, such that $|\Lambda A_{v,\Omega}| \gg 2JB_v$, where $A_{v,\Omega}$ is the spin-orbit coupling constant [see Eq. (A1b)], and B_v is the rotational constant for the vth vibrational state [63,64]; for NO, Gallagher *et al.* [25] give $A_{0,1/2}/B_0 \approx 75$.

For any molecule in a rovibronic state with $|\Lambda|>0$, the molecular energies (for fixed Λ, Σ, Ω, v, J, and laboratory-frame projection quantum number M_J) are twofold degenerate because the electronic Hamiltonian is invariant under re-

flection in a plane that contains the internuclear axis. The *rotational* Hamiltonian, however, perturbs these electronic states, shifting their energies and lifting this degeneracy. In NO the rotational Hamiltonian couples the $^2\Pi_{1/2}$, $^2\Pi_{3/2}$, and $^2\Sigma_{1/2}$ rovibronic states so that the actual ground state is a superposition of these states [34,65–67]. This coupling results in a splitting of each rotational level (of a particular vibrational manifold) into two nearly degenerate levels with opposite total parity. It also causes a breakdown of the Hund's case (a) description [24,62,64–66]. The rotational $^2\Pi_{1/2}$ states of NO are more accurately described by case a_β, "an intermediate case, slightly removed from Hund's case (a)" [26]. The pure Hund's case (a) description, however, is accurate for the $^2\Pi_{3/2}$ state because of the comparatively small [28] influence of the rotational Hamiltonian (see Sec. 8 of Ref. [68]).

Due to mixture of $\pm\Lambda$ states, each $2(2J+1)$-fold degenerate rovibronic energy level splits into two closely spaced $(2J+1)$-fold degenerate sublevels. This Λ-*doublet splitting* was first observed in NO in microwave measurements of pure rotational spectra by Burrus and Gordy [24]. The resulting sublevels of the Λ doublet are most often labeled e and f [69,70]. The splitting between these sublevels due to the rotational Hamiltonian increases with increasing J, accelerating the transition from Hund's case (a) to (b) as J increases. The Λ doublet splitting for the lowest rovibronic level of the $^2\Pi_{1/2}$ state is shown (on an expanded scale) in Fig. 1(b).

In analyses of pure rotational spectra [24–26,28] or of weak-field Stark-effect measurements of the dipole moment of NO [27,29], one must take into account magnetic hyperfine effects. Typical zero-field hyperfine splittings for NO [29] range from 0.0013 to 0.0027 cm^{-1}. But this energy range corresponds to trap depths of a few μK, which is much lower than the depth of current Stark traps for molecules [7]. Hence we shall neglect nuclear spin and hyperfine coupling.

A. The zero-field molecular states and energies of NO

The zero-field stationary states and energies of diatomic radicals of the class to which NO belongs are well-known [108]; relevant definitions and notation are summarized in the Appendix. This section gives the final equations we used in the present analysis.

To calculate the Λ-doublet splitting one should use the e/f-symmetrized molecular functions in Eq. (A6b) [23,68,71], since the L-uncoupling operator of Eq. (A8) does not mix e and f states. In an analysis of the Stark effect, these rotationless parity labels therefore pertain to the zero-field states of the Λ doublet (see Sec. III). In NO the perturbing $^2\Sigma_{1/2}$ state lies *above* the $^2\Pi$ state [67]. Both the e and f levels are *lowered* by the L-uncoupling operator, but not by the same amount; Geuzebroek *et al.* [72] have unambiguously verified by two experiments that, as illustrated in Fig. 1(b), the e state (which for the lowest rotational state has total parity $\pi=+1$) lies *below* the f state ($\pi=-1$).

The splitting between the energy levels of the Λ doublet,

$$\Delta\epsilon^{fe}_{v,J,\Omega} \equiv \epsilon^{f}_{v,J,\Omega} - \epsilon^{e}_{v,J,\Omega} > 0, \tag{1a}$$

is given to second order in the L-uncoupling operator by [25,68,73,74]

TABLE I. Molecular constants in cm^{-1} for the $^2\Pi$ levels of $^{14}N^{16}O$. Data from Refs. [74,76–78]. For variations in measured spectroscopic constants, see [79]. For further references, see footnotes to the table on $^{14}N^{16}O$ in Huber and Herzberg [76].

Physical significance	Symbol	Value (cm^{-1})
Rotational constant at equilibrium	$B_e(^2\Pi_{3/2})$	1.72016
	$B_e(^2\Pi_{1/2})$	1.67195
Centrifugal distortion constant	$D_e(^2\Pi_{3/2})$	10.2×10^{-6}
	$D_e(^2\Pi_{1/2})$	5.36×10^{-6}
Rovibrational interaction constant	$\alpha_e(^2\Pi_{3/2})$	0.0182
	$\alpha_e(^2\Pi_{1/2})$	0.0171
Harmonic angular frequency	$\omega_e(^2\Pi_{3/2})$	1904.04
	$\omega_e(^2\Pi_{1/2})$	1904.20
Anharmonicity constant	$\omega_e x_e(^2\Pi_{3/2})$	14.100
	$\omega_e x_e(^2\Pi_{1/2})$	14.075

$$\Delta\epsilon^{fe}_{v,J,1/2} = p_e\left(J+\frac{1}{2}\right) \quad \text{for } ^2\Pi_{1/2}, \tag{1b}$$

$$\Delta\epsilon^{fe}_{v,J,3/2} = q_v\left(J^2-\frac{1}{4}\right)\left(J+\frac{3}{2}\right) \quad \text{for } ^2\Pi_{3/2}. \tag{1c}$$

The constants p_v and q_v are defined in terms of the spin-orbit constant, the rotational constants, and the separation in energy $\Delta E^{\Sigma,\Pi} \equiv E_\Sigma - E_\Pi > 0$ between the $X\,^2\Pi$ term and the *higher-lying* perturbing $A\,^2\Sigma_{1/2}$ term as [65,66]

$$p_v \equiv \frac{4A_{v,3/2}B_v}{\Delta E^{\Sigma,\Pi}} \quad \text{for } ^2\Pi_{1/2}, \tag{2a}$$

$$q_v \equiv \frac{8B_v^2}{A_{v,3/2}\Delta E^{\Sigma,\Pi}} \quad \text{for } ^2\Pi_{3/2}. \tag{2b}$$

These expressions assume that the shapes of the $X\,^2\Pi$ and $A\,^2\Sigma_{1/2}$ potential energy curves are identical and hence that these states have the same vibrational wave functions, an approximation that is valid for NO [75]. (For details concerning the effect of Λ doubling on rotational states in the $^2\Pi$ states, see Table III of Ref. [26].) Taking into account the Λ-doublet splitting, the zero-field rovibronic energies are [see also Eq. (3.5) of Ref. [25]]

$$\epsilon^{e/f}_{v,J,\Omega} = \epsilon_{v,J,\Omega} \pm \frac{1}{2}\Delta\epsilon^{fe}_{v,J,\Omega}, \tag{3}$$

where $\epsilon_{v,J,\Omega}$ is the Born-Oppenheimer rovibronic energy (A9), $\Delta\epsilon^{fe}_{v,J,\Omega}$ is the Λ-doublet splitting of Eq. (A9), and the $+$ and $-$ signs correspond to the f and e states, respectively.

B. Molecular data for NO

The molecular constants required to evaluate the zero-field energies Eq. (A9) are identified and their measured values given for NO in Table I. In addition to these constants, one requires values for the spin-orbit constants of Eq. (A1a).

TABLE II. Experimental (E) and theoretical (T) values for vibrationally averaged dipole moments in the ground and first-excited vibrational states in the $^2\Pi$ spin-orbit states of $^{14}N^{16}O$. Values are given in Debye, where 1 D=3.335 64$\times 10^{-30}$ cm^{-1}. Note that experimental measurements yield only $|\mu_{v,\Omega}|$.

Source	$\mu_0(D)$	$\mu_1(D)$
(E) Liu *et al.* [89]	0.1595(15)	0.1425(16)
(E) Burrus and Graybeal [27]	0.158±0.006	
(E) Neumann [84]	0.15782±0.0002	
(E) Hoy *et al.* [29]	0.1574	0.1416
(T) Billingsley [85]	−0.139	−0.119
(T) Langhoff *et al.* [87]	−0.169	−0.152
(E) Rawlins *et al.* [88]	−0.1588	−0.1406

Hallin *et al.* [80] experimentally determined the spin-orbit constants for low-lying vibrational states of the $^2\Pi_{3/2}$ level; for the ground and first vibrational states, they obtained $A_{0,3/2}$=123.139 07(25) cm^{-1} and $A_{1,3/2}$ =122.894 90(27) cm^{-1} (see Refs. [28,60,78,81]). The corresponding *equilibrium* spin-orbit constant for the ground electronic state is [76] $A_{3/2}(R_e$=1.150 77 Å)=119.82 cm^{-1}. The separation between the interacting $^2\Pi$ and $^2\Sigma_{1/2}$ Born-Oppenheimer electronic states is [59] $\Delta E^{\Sigma,\Pi}$=43 966 cm^{-1}.

The constant p_v in the Λ-doublet splitting energy (1) depends on the vibrational state. One can experimentally determine this splitting from the frequency separation of Λ-doublet spectral lines for rotational transitions $J \rightarrow J+1$. From analysis of high-resolution Fourier spectra, Amiot *et al.* [82] (corrected in Table III of Ref. [83]) determined the values p_0=0.011 6893(80) cm^{-1} and p_1 =0.011 6878(14) cm^{-1} (for related determinations see Refs. [24,25,28,35,83]). For the Λ-doublet parameters of the $^2\Pi_{3/2}$ level, these authors obtained $q_0=9.507(74)\times 10^{-6}$ cm^{-1} and $q_1=9.443(68)\times 10^{-6}$ cm^{-1}. The resulting Λ-doublet splittings are in good accord with the theoretical calculations of [67], who discuss the theoretical underpinnings of this phenomenon and the wide variation in contemporary experimental values of q_v (see also Refs. [29,65,66]).

C. Dipole moments for NO

To evaluate the Stark shifts, we require the vibrationally averaged dipole moments for the $v=0$ and $v=1$ states of the spin-orbit state of interest. This quantity, the permanent electric dipole moment in the vth vibrational state [70]

$$\mu_{v,\Omega} \equiv \langle \alpha, v, S, \Lambda, \Sigma, \Omega, J, M_J | \mu | \alpha, v, S, \Lambda, \Sigma, \Omega, J, M_J \rangle, \quad (4)$$

depends on the magnitude but not on the sign of Ω. The permanent dipole moment for the $^2\Pi_{1/2}$ state of $^{14}N^{16}O$ has been measured, calculated, and discussed extensively; key results appear in Table II. The experimental results in this table come from microwave spectra except the value of Neumann [84], which was determined using a molecular-beam resonance technique. These measurements cannot determine the *sign* of $\mu_{v,\Omega}$. But the calculations of Billingsley [85], who used the optimized-valence-configuration multiconfiguration self-consistent-field method, show the polarity of the ground state to be N^-O^+, i.e., the dipole moment points from the nitrogen nucleus to the oxygen nucleus and therefore, by definition, is negative. This finding explains the signs in Table II. The more recent calculations of Refs. [86,87] entail multireference singles-plus-doubles configuration-interaction calculations. The values we use in the calculations of Sec. IV are those of Rawlins *et al.* [88]. These authors analyzed experimental data for vibrational-transition branching ratios, previous measurements of the static dipole moment, and absorption coefficients for transitions from the ground to the first vibrational state. They then used a nonlinear least-squares fit to determine a dipole moment function $\mu_\Omega(R)$, from which they calculate the vibrationally averaged moments in Table II.

III. THEORY: THE STARK EFFECT FOR NO

We here summarize the application of the two-state model and the standard perturbation-theory approximates to NO. For a static, homogeneous external electric field of strength $\mathcal{E}$ that points along the laboratory-frame Z axis, the Stark Hamiltonian is

$$\hat{\mathcal{H}}^{\mathcal{E}} = -\boldsymbol{\mu} \cdot \mathcal{E} = -\mu \mathcal{E} \cos\theta, \quad (5)$$

where $\boldsymbol{\mu}$ is the permanent dipole moment of the molecule, and θ is the polar angle of the field axis with respect to the internuclear axis. We require the matrix of this Hamiltonian in a basis defined by the two states of NO that are relevant to the experiments under consideration.

Symmetry properties of the Stark Hamiltonian $\hat{\mathcal{H}}^{\mathcal{E}}$ facilitate calculating its effect on the zero-field NO energies. Since $\hat{\mathcal{H}}^{\mathcal{E}}$ commutes with $\hat{J}_z$, it does not couple states of different $|\Omega|$; nor does it couple a state with $+\Omega$ to the corresponding state with $-\Omega$. Therefore in the rovibronic basis defined by Eq. (A2), whose elements we will here abbreviate as $|\Omega\rangle$, the matrix representation of the Stark Hamiltonian is diagonal:

$$\mathbf{H}^{\mathcal{E}}_{\{|\Omega\rangle\}} = \begin{pmatrix} \langle\Omega|\hat{\mathcal{H}}^{\mathcal{E}}|\Omega\rangle & 0 \\ 0 & -\langle\Omega|\hat{\mathcal{H}}^{\mathcal{E}}|\Omega\rangle \end{pmatrix}, \quad (6a)$$

where we have exploited the symmetry of the molecule to relate the (nonzero) diagonal elements [23]. But the Stark Hamiltonian does couple the e and f states defined in Eq. (A6b), which we will here abbreviate by $|e/f\rangle$. In this basis the diagonal matrix elements of $\hat{\mathcal{H}}^{\mathcal{E}}$ are zero, so the matrix representation is

$$\mathbf{H}^{\mathcal{E}}_{\{|e/f\rangle\}} = \begin{pmatrix} 0 & \langle e|\hat{\mathcal{H}}^{\mathcal{E}}|f\rangle \\ \langle e|\hat{\mathcal{H}}^{\mathcal{E}}|f\rangle & 0 \end{pmatrix}, \quad (6b)$$

where we have used the Hermiticity of $\hat{\mathcal{H}}^{\mathcal{E}}$ to equate the (nonzero) off-diagonal elements.

The sole matrix element $\langle\Omega|\hat{\mathcal{H}}^{\mathcal{E}}|\Omega\rangle$ needed to construct the representation (6a) of $\hat{\mathcal{H}}^{\mathcal{E}}$ in the $|\Omega\rangle$ basis is [23]

$$H^{\mathcal{E}}_{v,J,M_J,\Omega} = \langle \alpha, v, S, \Lambda, \Sigma, \Omega, J, M_J | \hat{\mathcal{H}}^{\mathcal{E}} | \alpha, v, S, \Lambda, \Sigma, \Omega, J, M_J \rangle \tag{7a}$$

$$= -\mathcal{E}\mu_{v,\Omega} \langle J, M_J, \Omega | \cos\theta | J, M_J, \Omega \rangle, \tag{7b}$$

where $|J, M_J, \Omega\rangle$ is the rotational eigenstate in Eq. (A2) and $\mu_{v,\Omega}$ is the vibrationally averaged dipole moment defined in Eq. (4). Since the laboratory-frame polar angle θ is the direction cosine $\boldsymbol{\alpha}^z_Z$, the diagonal matrix element of this quantity with respect to the rotational state $|J, M_J, \Omega\rangle$ is the expectation value of $\boldsymbol{\alpha}^z_Z$ in this state, the value of which is (see Sec. 3.9 and Table 3.2 of Ref. [69])

$$\langle J, M_J, \Omega | \boldsymbol{\alpha} | J, M_J, \Omega \rangle = \langle \boldsymbol{\alpha}^z_Z \rangle = \frac{\Omega M_J}{J(J+1)}. \tag{8}$$

The Stark matrix element (7a) is therefore

$$H^{\mathcal{E}}_{v,J,M_J,\Omega} = -\mu_{v,\Omega}\mathcal{E}\frac{\Omega M_J}{J(J+1)}, \quad M_J = -J, \ldots, +J. \tag{9}$$

A. The Stark effect in a two-state model

Although the zero-field Born-Oppenheimer states $|\alpha, v, S, \Lambda, \Sigma, \Omega, J, M_J, e/f\rangle$ are not degenerate, the Λ-doublet splitting in NO is so small that these states are well-separated in energy from all other rovibronic states [see Fig. 1(a)]. [This feature has been verified experimentally by Gallagher and Johnson [26] and by Hoy *et al.* [29] (see also Refs. [22,23]).] Moreover, applied fields in current cold molecular experiments are sufficiently strong that the product $\mu_{v,\Omega}\mathcal{E}$ is much larger than the hyperfine splitting [90]—conditions that bring into question the suitability of perturbation theory. Under these circumstances, we can determine the Stark energies by modeling the molecule as a two-state system [47,91]. We shall show in Sec. IV, such a *nonperturbative* approach is required for field strengths larger than a few kV/cm because second-order perturbation theory, which leads to the familiar "quadratic Stark effect" [22,29], is highly inaccurate for these field strengths.

We now define the two states in the present application of this model. The states $|\alpha, v, S, \Lambda, \Sigma, \Omega, J, M_J, e/f\rangle$ of Eq. (A6b) for fixed v, J, Λ, Σ, and Ω constitute a basis of $2(2J+1)$ eigenvectors in which we can expand the desired eigenvector of the total Hamiltonian $\hat{\mathcal{H}} = \hat{\mathcal{H}}^0 + \hat{\mathcal{H}}^{\mathcal{E}}$ (see the Appendix). Since $\hat{\mathcal{H}}^{\mathcal{E}}$ commutes with $\hat{J}_Z$, the Hamiltonian matrix in this basis is block diagonal with respect to the magnetic quantum number M_J. Hence we can consider each 2×2 submatrix for fixed M_J separately and obtain the eigenvalues of $\hat{\mathcal{H}}$ by diagonalizing [92]

$$\mathsf{H}_{\{|e/f\rangle\}} = \begin{pmatrix} H_{ee} & H_{ef} \\ H_{fe} & H_{ff} \end{pmatrix} = \begin{pmatrix} \epsilon^e_{v,J,\Omega} & \langle e|\hat{\mathcal{H}}^{\mathcal{E}}|f\rangle \\ \langle e|\hat{\mathcal{H}}^{\mathcal{E}}|f\rangle & \epsilon^f_{v,J,\Omega} \end{pmatrix}, \tag{10}$$

where the second equality follows from the symmetry properties of the e/f basis (Sec. III). The diagonal elements in $\mathsf{H}_{\{|e/f\rangle\}}$ are just the zero-field energies of the e and f states given in Eq. (3). By Hermiticity of $\hat{\mathcal{H}}$ the off-diagonal elements in this matrix are equal: $H_{fe} = H_{ef}$. By orthonormality of the e/f states, these elements are $H_{ef} = \langle e|\hat{\mathcal{H}}^0 + \hat{\mathcal{H}}^{\mathcal{E}}|f\rangle = \langle e|\hat{\mathcal{H}}^{\mathcal{E}}|f\rangle$. To evaluate H_{ef} we use Eq. (A6b) to express the off-diagonal matrix element in terms of the $\{|\Omega^{\pm}\rangle\}$ basis states. According to Eq. (6a), the matrix $\mathsf{H}^{\mathcal{E}}_{\{|\Omega^{\pm}\rangle\}}$ is diagonal. So the matrix element simplifies to the one already evaluated in Eq. (9):

$$\langle e|\hat{\mathcal{H}}^{\mathcal{E}}|f\rangle = \langle \Omega|\hat{\mathcal{H}}^{\mathcal{E}}|\Omega\rangle = H^{\mathcal{E}}_{v,J,M_J,\Omega} = -\mu_{v,\Omega}\mathcal{E}\frac{\Omega M_J}{J(J+1)}. \tag{11}$$

Diagonalizing the matrix (10) yields the Stark energies in the two-state model,

$$E^{e/f}_{v,J,M_J,\Omega} = \frac{1}{2}(\epsilon^e_{v,J,\Omega} + \epsilon^f_{v,J,\Omega}) \pm \frac{1}{2}\sqrt{4|H^{\mathcal{E}}_{v,J,M_J,\Omega}|^2 + (\Delta\epsilon^{fe}_{v,J,\Omega})^2}, \tag{12a}$$

where the + sign corresponds to the f state and the − sign to the e state. Noting from Eq. (3) that the average of the e and f zero-field energies is just the rovibronic energy $\epsilon_{v,J,\Omega}$ of Eq. (A9), and defining the two-state Stark shift

$$\Delta E^{e/f}_{v,J,M_J,\Omega} = \frac{1}{2}\sqrt{4|H^{\mathcal{E}}_{v,J,M_J,\Omega}|^2 + (\Delta\epsilon^{fe}_{v,J,\Omega})^2}, \tag{12b}$$

we can write Eq. (12a) as

$$E^{e/f}_{v,J,M_J,\Omega} = \epsilon_{v,J,\Omega} \pm \Delta E^{\mathcal{E}}_{v,J,M_J,\Omega}. \tag{12c}$$

This form emphasizes that Eq. (12b) gives the Stark shifts to the zero-field Born-Oppenheimer rovibronic energies $\epsilon_{v,J,\Omega}$ of Eq. (A9), not to the e/f energies $\epsilon^{e/f}_{v,J,\Omega}$ of Eq. (3).

Equations (12) show that the Stark effect increases the energies of the upper (f) levels [see Fig. 1(b)] and decreases the energies of the lower (e) levels [90]. These shifts depend on the magnitude *but not on the sign* of M_J: that is, the Stark-shifted levels remain twofold degenerate. To calculate these shifts we require only the field strength and the (averaged) dipole moments in the relevant vibronic states (see Sec. II C).

B. Perturbation theory regained: The strong- and weak-field limits

Burrus and Graybeal [27] used Stark spectroscopy to measure the dipole moment for the $v=0$ vibrational state of the $^2\Pi_{1/2}$ level of $^{14}N^{16}O$. Subsequently, Hoy *et al.* [29] used laser Stark spectroscopy to measure $\mu_{v,\Omega}$ for the ground and first vibrational states and considered both $^2\Pi$ levels. As befits such microwave-spectroscopy experiments, these authors focused on the *weak-field limit*, included hyperfine splitting, and *used perturbation theory* [22,23] to calculate the quadratic (second-order) and linear (first-order) Stark shifts. We here give the equations of perturbation theory for NO as approximations to those of the two-state model [93].

Although we obtained the perturbation-theory approximates using standard perturbation theory, they can be math-

ematically related to the two-state results of Sec. III A by a series expansion of the exact result. We thus write the Stark energy levels of Eqs. (12) as

$$E^{e/f}_{v,J,M_J,\Omega} = \epsilon^{e/f}_{v,J,\Omega} \pm \left(\Delta E^{\mathcal{E}}_{v,J,M_J,\Omega} - \frac{1}{2}\Delta\epsilon^{fe}_{v,J,\Omega} \right). \tag{13}$$

In the presence of Λ doubling, *second-order perturbation theory is valid only if the external electric field is sufficiently weak*. In this weak-field limit the two-state Stark shift reduces to the familiar quadratic shift. Writing Eq. (13) as

$$E^{e/f}_{v,J,M_J,\Omega} = \epsilon^{e/f}_{v,J,\Omega} \pm \frac{1}{2}\Delta\epsilon^{fe}_{v,J,\Omega}\left[\sqrt{1+4\left(\frac{H^{\mathcal{E}}_{v,J,M_J,\Omega}}{\Delta\epsilon^{fe}_{v,J,\Omega}}\right)^2} - 1 \right], \tag{14a}$$

we expand the square root in the small parameter $|H^{\mathcal{E}}_{v,J,M_J,\Omega}/\Delta\epsilon^{fe}_{v,J,\Omega}|$ *and retain only the first term* to obtain

$$E^{e/f}_{v,J,M_J,\Omega} \approx \epsilon^{e/f}_{v,J,\Omega} \pm E^{(2)}_{v,J,M_J,\Omega}, \tag{14b}$$

where the plus and minus signs refer to the *f* and *e* states, respectively, and we have identified the *second-order* correction term as the quadratic Stark shift to the zero-field *e*/*f* energies:

$$E^{(2)}_{v,J,M_J,\Omega} = \frac{[E^{\mathcal{E}}_{v,J,M_J,\Omega}(\mathcal{E})]^2}{\Delta\epsilon^{fe}_{v,J,\Omega}}. \tag{15}$$

For the second-order approximation to the Stark shift to be accurate, the applied field must be weak enough that

$$|H^{\mathcal{E}}_{v,J,M_J,\Omega}(\mathcal{E})| \ll \frac{1}{2}\Delta\epsilon^{fe}_{v,J,\Omega}. \tag{16}$$

In the other extreme—the *strong-field limit*, where the field is strong enough to render the Λ-doublet splitting negligible—Eq. (12c) reduces to

$$E^{e/f}_{v,J,M_J,\Omega} = \epsilon^{e/f}_{v,J,\Omega} \pm H^{\mathcal{E}}_{v,J,M_J,\Omega} = \epsilon^{e/f}_{v,J,\Omega} \mp \mu_{v,\Omega}\mathcal{E}\frac{\Omega M_J}{J(J+1)}. \tag{17}$$

The second term in this result agrees with the first-order (linear) Stark shift [22],

$$E^{(1)}_{v,J,M_J,\Omega} = \langle\Omega|\hat{\mathcal{H}}^{\mathcal{E}}|\Omega\rangle = -\mu_{v,\Omega}\mathcal{E}\frac{\Omega M_J}{J(J+1)}, \tag{18}$$

which one obtains by neglecting the Λ doublet splitting altogether [29].

To conclude we write our equations for the Stark shifts in a form that is convenient for application to other molecules and for the comparisons of Sec. IV. To this end we introduce the dimensionless variable

$$\eta \equiv \frac{H^{\mathcal{E}}_{v,J,M_J,\Omega}}{\Delta\epsilon^{fe}_{v,J,\Omega}}, \tag{19}$$

which is the Stark matrix element for an arbitrary rovibronic state normalized to the splitting of the Λ doublet. In terms of this variable, Eqs. (12b), (15), and (18) for the Stark shifts become

$$\Delta E^{\mathcal{E}}_{v,J,M_J,\Omega} = \pm\sqrt{\frac{1}{4}+\eta^2}, \tag{20a}$$

$$E^{(2)}_{v,J,M_J,\Omega} = \pm\left(\frac{1}{2}+\eta^2\right), \tag{20b}$$

$$E^{(1)}_{v,J,M_J,\Omega} = \pm\left(\frac{1}{2}+\eta\right), \tag{20c}$$

where the + and − signs refer to the *f* and *e* states, respectively. Note that because η is defined in terms of the matrix element $H^{\mathcal{E}}_{v,J,M_J,\Omega}$, this variable depends on the field strength and on the rovibronic state under consideration. Equations (20) are "generic" expressions for the Stark shifts, applicable to any molecule with a $^2\Pi$ ground state under conditions where hyperfine effects are negligible.

C. Assessing perturbative treatments of the Stark effect

In the preceding section, we described three ways to calculate Stark shifts for any molecule with $|\Lambda| > 0$ that is well-represented by Hund's case (a) under conditions where hyperfine structure is negligible. Three points are relevant to these comparisons.

(1) The linear Stark shift [Eq. (14b)] results from first-order perturbation theory; this result is valid only when the Stark interaction energy is large compared to the Λ-doublet splitting.

(2) The quadratic Stark shift [Eq. (15)] results from second-order perturbation theory and assumes that the Stark energy is small compared to the Λ-doublet splitting. When this approximation holds, the first-order Stark shift is zero.

(3) The two-state model diagonalizes the Hamiltonian, assuming only that the Λ-doublet splitting and Stark interaction energies are small compared to the separation of the rovibronic level under consideration from other levels.

In Fig. 2(a), we plot the Stark shifts for the ground rovibronic state ($v=0, J=1/2$) of the $^2\Pi_{1/2}$ spin-orbit level as a function of field strength. This figure shows significant differences between the quadratic Stark shift and that of the two-state theory—even for relatively low electric fields. According to perturbation theory, the second-order correction lowers the energies of *e* states and raises the energies of *f* states. Qualitatively this behavior is the same as that of the two-state Stark shifts. Quantitatively, however, the condition (16) breaks down at field strengths above a few kV/cm. (The linear approximation is not expected to be accurate at low field strengths; it is valid only for Stark shifts greater than the Λ-doublet splitting.) To quantify the implications of Figs 2(a), we compare in Table III Stark shifts for the *f* state from the (very low) field strengths at which the quadratic shift is accurate to the (very high) strength at which the linear approximation holds.

In Figs 2(b), we compare the fractional difference between the linear and quadratic Stark shifts of Eqs. (20) to those of the two-state model. Since the dimensionless vari-

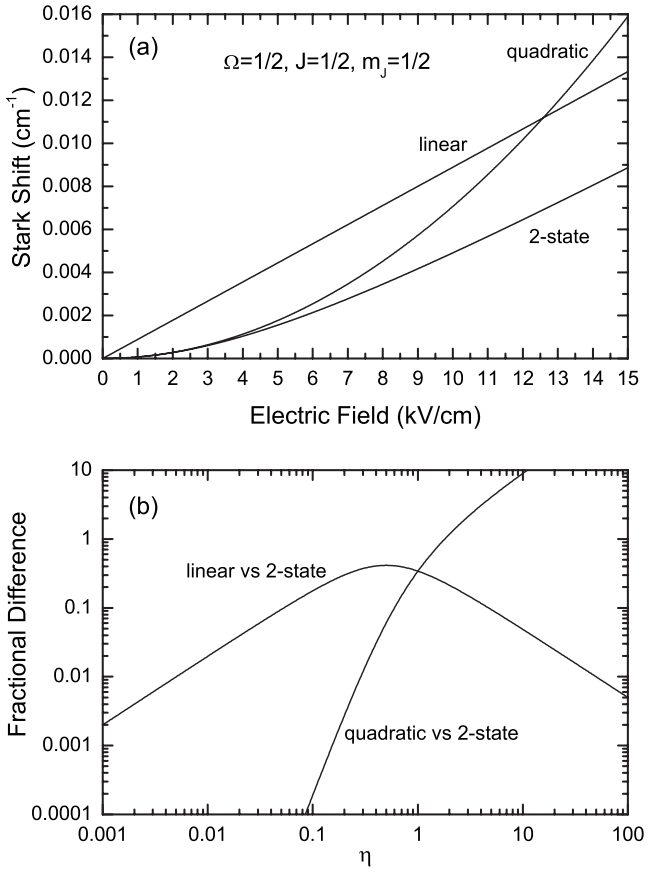

FIG. 2. (a) The dc Stark shifts for the $v=0$, $J=1/2$ state of the $^2\Pi_{1/2}$ spin-orbit level as a function of electric field strength. Shifts in the two-state model and in first- and second-order perturbation theory are shown over an experimentally realistic range of field strengths. (b) The fractional difference between Stark shifts, as calculated using perturbation theory and using the two-state model [see Eqs. (20)], for a rovibronic state of a Hund's case (a) molecule. First- and second-order perturbation theory give the linear and quadratic approximations, respectively. The parameter η, the Stark matrix element normalized to the Λ-doublet splitting, is defined in Eq. (19).

able η of Eq. (19) depends on the dipole moment, electric field, and quantum state, these curves show the relative accuracy of perturbation theory for any rovibronic state of any radical that can be treated in Hund's case (a) when hyperfine effects are negligible. Especially noteworthy is the striking, rapid increase in the error of the quadratic Stark shift around $\eta=1$.

To illustrate the behavior of Stark shifts over the range of field strength that is experimentally accessible for electrostatic trapping, we show in Fig. 3 results from the two-state model for the $J=1/2$ and $J=3/2$ rotational levels of the $^2\Pi_{1/2}$ state and for the $J=3/2$ and $J=5/2$ levels of the $^2\Pi_{3/2}$ state. In both cases we consider the ground vibrational manifold ($v=0$). Since the Stark energies depend on the magnitude but not the sign of M_J, each Stark-shifted level remains twofold degenerate. Because the Λ-doublet splitting is so small for $^2\Pi_{3/2}$ states, the Stark shift for these states is essentially linear over the entire range of field strengths of interest. For the $J=3/2$ state of the $^2\Pi_{1/2}$ level, the Stark

TABLE III. Comparison of two-state, quadratic, and linear Stark shifts in cm^{-1} for the $v=0$, $J=1/2$, $M_J=1/2$ zero-field energy of the e state of the $^2\Pi_{1/2}$ level in NO as a function of electric field strength $\mathcal{E}$ in kV/cm. The "linear" column gives the Stark shift [18] obtained by neglecting the splitting of the Λ doublet compared to the Stark matrix element [9]. Field strengths were chosen to illustrate the breakdown of the linear and quadratic approximations.

$\mathcal{E}$ (kV/cm)	Two-state	Quadratic	Linear
0.5	0.00002	0.00002	0.00044
2.0	0.00026	0.00027	0.00178
5.0	0.00150	0.00169	0.00444
10.0	0.00479	0.00676	0.00889
20.0	0.01287	0.02704	0.01778
50.0	0.03898	0.16897	0.04444
100.0	0.08323	0.67589	0.08889
300.0	0.26088	6.08300	0.26666
500.0	0.43862	16.8970	0.44443
1000.0	0.88303	67.5890	0.88886

energy at 40 kV/cm is more than half of the energy of the Λ doublet, and Fig. 2(b) shows that as the field strength increases, second-order perturbation theory rapidly and significantly breaks down. Indeed, for the $J=1/2$ rotational state of this level, this approximation is invalid for most relevant trapping fields.

IV. EXPERIMENT: PRODUCING COLD NO MOLECULES WITH A STARK GUIDE

One way to produce cold samples of atoms and molecules is to select the cold fraction ($T \leqslant 1$ K) of molecules in the Maxwell-Boltzmann speed distribution that emerges from a thermal source. In this approach an atomic or molecular beam is directed into a two-dimensional guide that is bent at an angle such that there is no line-of-sight between the input and output ends of the guide. This guide transmits only particles that move slowly enough to be repelled from the walls by magnetic or electric fields and guided. The feasibility of this method has been demonstrated for Li [94], Rb [95], and H_2CO and ND_3 [96].

In our experimental study of the feasibility of using such a device to produce cold NO we inject NO molecules from an effusive source at 77 K into a *straight* hexapole Stark guide. As illustrated in Fig. 4(a), in this apparatus there does exist a line-of-sight between the input and the output. The hexapole guide, a cross section of which is shown in Fig. 4(b), consists of six wires, with positive and negative voltages placed on alternating wires, and produces electric fields as high as 65 kV/cm. Although our objectives are different, our NO guide is functionally identical to the hexapole NO guide used by Stolte and co-workers [97,98]. The primary difference is that we use a 77 K effusive source, while Stolte and co-workers used a molecular-beam source. The electric field inside the guide is not azimuthally symmetric. Along the circle that defines the highest edge values of the guide

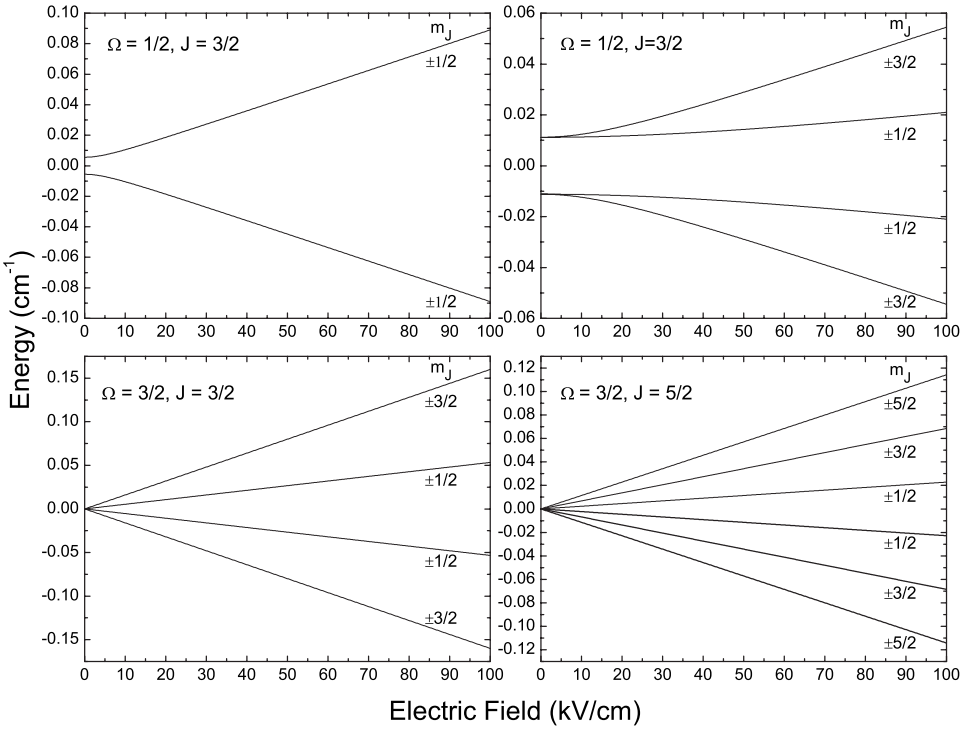

FIG. 3. The dc Stark shifts for the two lowest rotational levels of the ground vibrational manifold of the $\Omega=1/2$ and $\Omega=3/2$ states of $^{14}N^{16}O$ as a function of the strength of the applied electric field. In each case, the states whose energies increase with increasing field strength correspond to the zero-field f level of the Λ doublet. Those whose energies decrease with field strength correspond to the zero-field e level. The zero of energy is at the midpoint of the Λ doublet. (The Λ-doublet splitting for the $\Omega=3/2$ state is not visible on the scale of this figure.)

potential, the potential energy attains a minimum at each wire and a maximum halfway between each wire [Fig. 4(b)]. Calculating the electric field inside the guide, we find that the easiest escape route for the particles corresponds to a field strength of 35 kV/cm at a guide voltage of 4.5 kV.

Particles whose trajectories are not along a line-of-sight to the output will be guided to the output if their transverse kinetic energy is smaller than the energy of their Stark interaction with the electric field. Due to this collimation effect, the number of molecules at the output will be enhanced. Because the Stark interaction energy is small compared to the average thermal energy of the beam, only the cold fraction is collimated. Further details of the apparatus are described in Ref. [99].

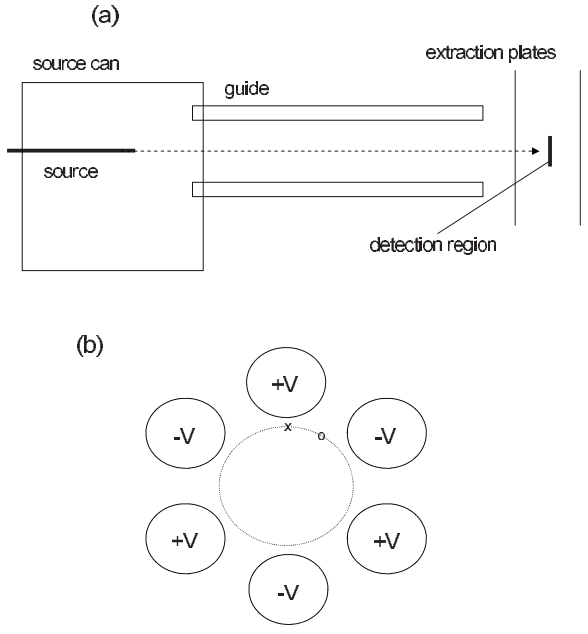

FIG. 4. (a) Schematic of the experimental apparatus (not to scale). (b) Cross section of the hexapole guide. The central circle defines the highest edge of the two-dimensional guide potential. On this central circle the cross and small open circle indicate points of lowest and highest guide potential, respectively, along the edge of the guide.

In the present experiments, we observe enhancement of the number of molecules in the lowest rovibrational state of $^{14}N^{16}O$. The particles are detected by exciting the transition $|X\,^2\Pi_{1/2},v=0,J=1/2\rangle \rightarrow |A\,^2\Sigma_{1/2},v=0,J=3/2,N=2\rangle$ at 226.180 nm [100]. The excited A state is then ionized with 327 nm laser radiation, and the resulting cations are detected on a microchannel plate. Because of drifts in laser intensity and flux from the source, constant normalization of the detected signal is necessary. To measure the effect of the guide on the molecular beam, the number of particles in the $|^2\Pi_{1/2},v=0,J=1/2\rangle$ state is measured as the guide voltage is increased from 0 to 4.5 kV.

We now present data for the enhancement of NO molecules due to passage through the Stark guide. Since this enhancement depends on the Stark interaction, we can use the variation of this quantity with guide voltage to assess the theoretical treatment in Sec. III in the context of experiments on cold molecules. Figure 5 shows the number of ions detected by the microchannel plate. Because fluctuations in the number of detected molecules were smallest at the highest count rates, we normalized the data in this figure to the number of ions detected with maximum voltage applied to the Stark guide, $V=4.5$ kV.

In each measurement we count the number of ions collected during 320 laser pulses with a particular voltage on the guide and divide the result by the corresponding number of ions for a voltage of 4.5 kV. In order to determine the statistical error we take ten consecutive measurements of this

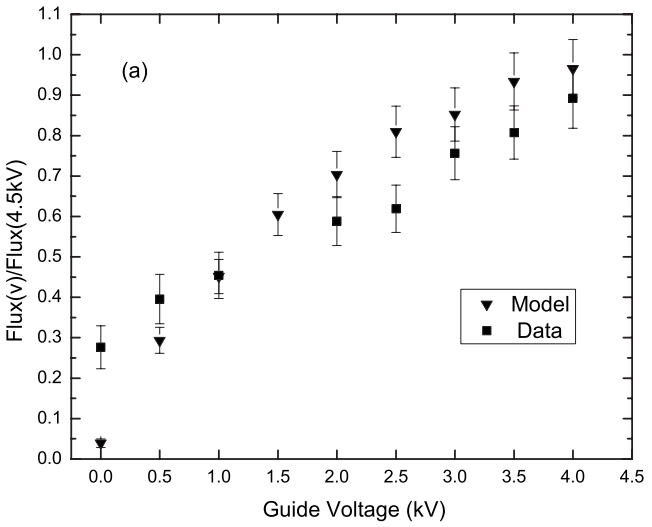

FIG. 5. The number of detected particles leaving the guide in the $J=1/2$ ground rovibrational state as a function of guide voltage. Comparison of results from the two-state model of Sec. III to measured data. The flux is normalized to the flux at the maximum voltage, 4.5 kV, and the data is compared to *normalized* fluxes calculated using two-state equations for the Stark shift. Note the discussion in the text of the effects of the normalization procedure used in generating this figure.

type. We then repeat this process on several days, adjusting the alignment of the ionizing lasers and the input pressure of NO in order to evaluate systematic errors in the apparatus. The data are subject to a systematic error that is comparable in magnitude to the statistical uncertainty, which we determine by comparing data taken with different configurations. We add the systematic error (in quadrature) to the statistical error to determine the error bars in Fig. 5(a), which correspond to a 2σ confidence interval.

We model the electric field $\mathcal{E}(\mathbf{r})$ using the numerical software program SIMION [101] including in the model file the conducting surfaces of the source can, the source tube, the guide, and the detection plates. Motion of particles in the guide is calculated by finding the force on the particles, $\mathbf{F}=-\boldsymbol{\nabla}U(\mathbf{r})$, where the potential energy $U(\mathbf{r})$ is given by the Stark shift $\Delta E^{\mathcal{E}}_{v,J,M_J,\Omega}$ of Eq. (12b) as determined using the two-state model of Sec. III A. [The dependence on $\mathbf{r}$ enters the Stark shift through the $\mathbf{r}$-dependent electric field strength, which appears in the matrix element of Eq. (11).] Only molecules in states whose energy increases with increasing electric field (so-called "low-field seeking states") are guided. From the potential energy $U(\mathbf{r})$ for our system we create an equivalent electric field for ion propagation in an identical geometry. The SIMION program calculates Monte Carlo trajectories of ions in arbitrary electric fields. So once we have found $U(\mathbf{r})$ for our system, we create an equivalent electric field for ion propagation. Thus the SIMION *ion*-trajectory simulator calculates our *neutral* particle trajectories.

In simulating the output of the guide, we assume that the source provides an isotropic angular distribution, although we considered only particles whose trajectories permitted them to enter the guide. In a previous measurement, we determined that the speed distribution is proportional to $v^2e^{-\alpha v^2}$ (where α is constant) as in a standard one-dimensional Maxwell-Boltzmann distribution. The expected speed distribution for the flux from an effusive source is proportional to v^3 [99]. The time during which laser radiation is on, however, is small compared to that required for the particles to undergo any significant movement. Therefore we measure the density directly. Assuming this speed distribution, we found the temperature of the gas to be 77 K, in agreement with a thermistor measurement of the temperature of the source tube. For each voltage on the guide we simulated 20 000 trajectories and counted the number of particles that were successfully guided into the detection region. The result of each simulation at each voltage was divided by the corresponding value for 4.5 kV; as noted above, this step normalizes the data. Thus no fitting parameters were involved in generating the comparison in Fig. 5.

The error bars for both the experiment and the Monte Carlo simulations represent a 2σ confidence interval. As Fig. 5 shows, the two-state model and the data disagree significantly only for a guide voltage of 0 kV. This disagreement most likely results from incomplete modeling of fringing fields at the input. At the input of the guide, a dielectric piece holds the wires in place. This piece will modify the fields at the entrance—an effect that cannot be easily simulated in SIMION. Note that this effect is present in all data, even the data at 0 kV, because these data are normalized to the output at 4.5 kV. Since improperly modeling the input fields will similarly affect data simulated at different voltages, the *largest* such effect will appear in data at 0 kV. Another possibility is a background signal in the data that would have the largest effect on the small signal comparison at 0 kV. We conclude that the results from the two-state model are consistent with the measured data over the range of voltages considered.

V. CONCLUSIONS

In previous literature concerning NO, the Stark effect for $^2\Pi_{3/2}$ states has been often described as "linear" and that for $^2\Pi_{1/2}$ states as "quadratic." Each of these characterizations implies a particular *perturbative* model. We have demonstrated the extent to which *for field strengths which are relevant to trapping cold NO* these characterizations and the assumptions inherent in them are unsuitable.

The Stark shifts of perturbation theory (Sec. III B) are mathematical approximations (in the strong- and weak-field limits) to the Stark shifts of the nonperturbative two-state model of Sec. III A. The numerical comparisons of Sec. III C quantify the validity of these approximations for NO molecules at field strengths from 0 to 15 kV/cm and show the magnitude of the error that perturbative approximations introduce into calculated Stark shifts.

The experimental aspect of this work considers the validity of the two-state model itself. The relative isolation of the states of interest in the present work on NO from other states of the molecule, and the small magnitude of (neglected) hyperfine interactions give reason for optimism. The experimental data reported in Sec. IV and the simulations in Fig. 5 show that for NO in its ground state, the two-state model is

accurate for applied electric field strengths on the order of 100 kV/cm. In Figs. 2 and 3 these equations are applied to the *class* of radicals to which NO belongs [102].

Because the two-state model is not significantly more complicated and does not break down in the relevant range of experimental fields, we recommend that the two-state model be used except where compelling reasons argue for the perturbation-theory alternative (see, for example, [37]), and that extreme care be exercised if the further simplification of perturbation theory is desired.

We hope that these quantitative assessments along with our two-state equations for the Stark shifts, used in conjunction with Eqs. (A9) for the rovibronic energies (including spin-orbit and spin-uncoupling effects) and Eqs. (1) for the splitting of the Λ doublet, will constitute a reliable resource for cold-molecule experiments involving $^2\Pi$ molecules with an odd number of electrons.

ACKNOWLEDGMENTS

The authors are grateful to Jason Alexander for help with the numerical simulations, and to Dr. Gregory A. Parker and Dr. Jim Shaffer for useful suggestions for improving the manuscript. This project was supported in part by the U.S. National Science Foundation under Grant. No. PHY-0354858 and by the Office of Naval Research under Grant No. N00014-02-1-0601.

APPENDIX: ZERO-FIELD MOLECULAR STATES AND ENERGIES OF NO

We denote eigenvectors of the Born-Oppenheimer *electronic* Hamiltonian $\hat{\mathcal{H}}^{\mathrm{e}}$ by $|\alpha,S,\Lambda,\Sigma,\Omega,J\rangle$, where the (signed) quantum numbers Λ, Σ, and Ω refer to projections along the internuclear axis, the z axis of the molecular (body-fixed) coordinate system. The quantum number S corresponds to total electronic spin, and α denotes the electronic energy (e.g., X,A,a, etc.). For NO, which essentially belongs to Hund's case (a), the quantum number $\Omega \equiv \Lambda+\Sigma$ is redundant. It is useful, though, to include Ω as a state label because Ω identifies the sublevels that result from the spin-orbit interaction.

Absent spin-orbit interactions, the Born-Oppenheimer electronic energy $E^{(\mathrm{BO})}_{\Lambda,\Sigma}(R)$, the eigenvalue of $\hat{\mathcal{H}}^{\mathrm{e}}$ for electronic state $|\alpha,S,\Lambda,\Sigma,\Omega,J\rangle$, depends on the spin multiplicity $2S+1$ and on the magnitude—but not the sign—of Λ. For an arbitrary angular momentum coupling scheme, adding the spin-orbit Hamiltonian to $\hat{\mathcal{H}}^{\mathrm{e}}$ results in states in which neither Λ nor Σ are rigorously good quantum numbers. Since the sum $\mathbf{\Lambda}+\mathbf{\Sigma}$ is a constant of the motion, spin-orbit states are labeled by Ω. In the Hund's case (a) idealization, however, Σ and Λ remain good quantum numbers and are used as state labels [62,64,69]. For a $^2\Pi$ state, the allowed values of Ω are $\pm 1/2$ and $\pm 3/2$, but the spin-orbit energies depend only on the magnitude of Ω.

Neglecting second-order corrections (see Sec. 2.4.1 of Ref. [75]), the spin-orbit shifts to $E^{(\mathrm{BO})}_{\Lambda,\Sigma}(R)$ are the diagonal matrix elements of the spin-orbit Hamiltonian in the basis of Born-Oppenheimer electronic states. The first-order shift, written in terms of the spin-orbit coupling constant $A_\Omega(R)$, is

$$A_\Omega(R)\Lambda\Sigma = \langle \alpha,S,\Lambda,\Sigma,\Omega,J|\hat{\mathcal{H}}^{SO}|\alpha,S,\Lambda,\Sigma,\Omega,J\rangle. \tag{A1a}$$

The resulting fine-structure levels are equally spaced about the Born-Oppenheimer electronic energy. Following Huber and Herzberg [76], we choose the zero of energy at the lowest spin-orbit level of the ground electronic term at the equilibrium internuclear separation R_e. Thus $A_{1/2}(R_e)=0$, and the energy of the upper spin-orbit level is $A_{3/2}(R_e)>0$. When we include rovibrational motion, we measure spin-orbit level energies from the ground rovibrational state, so $A_{0,1/2}=0$.

Since the molecule vibrates, the actual spin-orbit constant is the average of $A_\Omega(R)$ over a vibrational state of the molecule,

$$A_{v,\Omega} = \langle v|A_\Omega(R)|v\rangle_R = A_\Omega(R_e) - \chi_e\left(v+\frac{1}{2}\right), \tag{A1b}$$

where the spectroscopic constant χ_e corrects the equilibrium spin-orbit coupling constant $A_\Omega(R_e)$ to allow for vibrational motion, and the subscript R signifies integration over the internuclear separation.

For a Hund's case (a) molecule the Born-Oppenheimer rovibronic states are represented by the direct products [73]

$$|\alpha,v,S,\Lambda,\Sigma,\Omega,J,M_J\rangle = |\alpha,S,\Lambda,\Sigma,\Omega,J\rangle \otimes |v\ J\rangle \otimes |J,M_J,\Omega\rangle. \tag{A2}$$

Here the vibrational state is denoted $|v,J\rangle$. The quantum number J corresponds to the angular momentum operator (sans nuclear spin), i.e., the sum of the total electronic angular momentum and the rotational angular momentum of the molecule $\mathbf{N}$ [103]

$$\hat{\boldsymbol{J}} \equiv \hat{\mathbf{L}} + \hat{\mathbf{S}} + \hat{\mathbf{N}}. \tag{A3}$$

The (symmetric top) rotational state $|J,M_J,\Omega|$ is an eigenvector of $\hat{J}^2$, $\hat{J}_Z$, and $\hat{J}_z$ (see Sec. 1.3.3 of Ref. [75]), where the subscripts Z and z refer to the polar axis of the (space-fixed) laboratory frame and the (body-fixed) molecular frame, respectively. Since rotation takes place in the plane of the internuclear axis, $\mathbf{N}$ is perpendicular to this axis. Hence the projection of $\mathbf{N}$ along the internuclear axis is zero, and the quantum number that corresponds to J_z is $\Omega=\Lambda+\Sigma$. The ket $|\alpha,S,\Lambda,\Sigma,\Omega,J\rangle$ is an eigenvector of the Born-Oppenheimer electronic Hamiltonian and that part of the rotational Hamiltonian [Eq. (A7b) below] whose matrix elements are diagonal [75],

$$\hat{\mathcal{H}}^{\mathrm{rot}}_{\mathrm{diag}}(R) \equiv \frac{1}{2\mu R^2}[(\hat{J}^2-\hat{J}_z^2)+(\hat{L}-\hat{L}_z^2)-(\hat{S}^2-\hat{S}_z^2)]. \tag{A4}$$

Because of the isotropy of free space, properly symmetrized eigenfunctions of the molecular Hamiltonian have well-defined total parity. In Born-Oppenheimer theory, these parity eigenfunctions are linear combinations of degenerate rovibronic stationary-state wave functions that have positive

and negative projection quantum numbers Ω (for fixed $\Omega \neq 0$).

These linear combinations are eigenfunctions of the vertical reflection operator $\hat{\sigma}_v(xz)$, where xz signifies a plane containing the internuclear axis (the z axis of the molecular reference frame) (see Chap. 9 of Ref. [70]). The operator $\hat{\sigma}_v(xz)$ inverts internal coordinates through the origin [61]. When $\hat{\sigma}_v(xz)$ acts on a *rovibronic state* $|\alpha,v,S,\Lambda,\Sigma,\Omega,J,M_J\rangle$, the resulting eigenvalues $\pi=\pm 1$ define the total parity of the state [104]. At first glance, it would seem easy to construct properly symmetrized rovibrational states by simply adding or subtracting states $|\alpha,v,S,\Lambda,\Sigma,\Omega J,M_J\rangle$ with positive and negative values of the angular-momentum projection quantum numbers:

$$|v,|\Lambda|,|\Sigma|,J,M_J,|\Omega|,\pi\rangle \frac{1}{\sqrt{2}}(|\alpha,v,S,\Lambda,\Sigma,\Omega,J,M_J\rangle \pm |\alpha,v,S,-\Lambda,-\Sigma,-\Omega,J,M_J\rangle). \quad \text{(A5)}$$

The problem is that it is not necessarily the case that the plus sign on the right-hand side of this linear combination corresponds to even parity ($\pi=+1$) and the minus sign corresponds to odd parity. Rather, the total parity of a group of energy levels, such as the upper and lower states of the Λ doublet, alternate with increasing J. In this alternation lies the usefulness of the e/f symmetry classification scheme: in this scheme the signifiers, such as $\pi(-1)^{J-1/2}$ for a molecule with an odd number of electrons, factor out this J-dependence and so are *independent of the rotational state of the molecule* [64]. The values of these signifiers are therefore referred to as the rotationless parity of the rovibronic state [105]. The e/f classification scheme of a rovibronic state gives no more information than the total-parity (π) scheme, but because the e/f scheme is "rotationless," it is much more convenient [106].

Except for molecules with an even number of electrons in an electronic state in which $\Lambda=\Omega=0$, construction of the e/f rovibronic eigenvectors proceeds in a straightforward manner depending on whether the molecule has an even or odd number of electrons. For a molecule such as NO that has an odd number of electrons in an electronic state with $|\Lambda|>0$, the properly symmetrized *rovibronic* states wave functions have the form [73,107,111,112]

$$|\alpha,v,S,\Lambda,\Sigma,\Omega,J,M_J,e/f\rangle = \frac{1}{\sqrt{2}}[|\alpha,v,S,\Lambda,\Sigma,\Omega,J,M_J\rangle \pm (-1)^{S+1}|\alpha,v,S,-\Lambda,-\Sigma,-\Omega,J,M_J\rangle], \quad \text{(A6a)}$$

where the plus yields an e state, and minus yields an f state. For NO in a $^2\Pi$ state $S=1/2$, so the e/f rovibronic states are

$$|\alpha,v,S,\Lambda,\Sigma,\Omega,J,M_J,e/f\rangle = \frac{1}{\sqrt{2}}(|\alpha,v,S,\Lambda,\Sigma,\Omega,J,M_J\rangle \pm |\alpha,v,S,-\Lambda,-\Sigma,-\Omega,J,M_J\rangle). \quad \text{(A6b)}$$

The rotational Hamiltonian lifts the degeneracy of the states (A6b).

In addition to the spin-orbit operator, electronic and rotational terms in the nonrelativistic molecular Hamiltonian can mix the Born-Oppenheimer states of Eq. (A2) and change the corresponding energies [69,75]. For the states and processes of interest here, these corrections are negligible except for those due to terms in the rotational Hamiltonian that induce the Λ-doublet splitting. The rotational Hamiltonian is

$$\hat{\mathcal{H}}^{\text{rot}} = \frac{1}{2\mu R^2}\hat{\mathbf{N}}^2, \quad \text{(A7a)}$$

where μ is the reduced mass of the molecule. With the definition (A3) this Hamiltonian assumes the form [75]

$$\hat{\mathcal{H}}^{\text{rot}} = \hat{\mathcal{H}}^{\text{rot}}_{\text{diag}} + \hat{\mathcal{H}}^{\text{SE}} + \hat{\mathcal{H}}^{\text{Sun}} + \hat{\mathcal{H}}^{\text{Lun}}, \quad \text{(A7b)}$$

where the part of $\hat{\mathcal{H}}^{\text{rot}}$ that is diagonal in the Hund's (a) basis is given by Eq. (A4). The operator $\hat{\mathcal{H}}^{\text{rot}}_{\text{diag}}$ does not couple different electronic states; its expectation value is just the rotational contribution to the energy of the state $|\alpha,v,S,\Lambda,\Sigma,\Omega,J,M_J\rangle$. Of the other terms, $\hat{\mathcal{H}}^{\text{SE}}$ is the spin-electronic term, which mixes states of the same Ω and S but different Λ and Σ, and $\hat{\mathcal{H}}^{\text{Sun}}$ is the spin-uncoupling term, which mixes states with different $|\Omega|$ that have the same Λ and S but different Σ (see Sec. 7 of Ref. [68]); this term contributes to the rotational energy [*vide infra* Eq. (A9) below] but does not split the Λ doublet. The third term, the L-uncoupling operator

$$\hat{\mathcal{H}}^{\text{Lun}} = -\frac{1}{2\mu R^2}(J^+L^- + J^-L^+), \quad \text{(A8)}$$

mixes different rovibronic states with the same Σ and S but different Λ and hence different Ω. Since $\hat{\mathcal{H}}^{\text{Lun}}$ couples states with $\Delta\Lambda=\pm 1$, $\Delta\Sigma=0$, and $\Delta\Omega=\pm 1$, this operator is responsible for splitting the Λ doublet.

In the Hund's case (a) basis $\{|\alpha,v,S,\Lambda,\Sigma,\Omega,J,M_J\rangle\}$, the Born-Oppenheimer rovibrational energy measured from $E=0$ at the ground rovibrational state of the lowest spin-orbit level is [25,28,59,71,74]

$$\epsilon_{v,J,\Omega} = A_{v,\Omega} + \omega_e\left(v+\frac{1}{2}\right) - \omega_e x_e\left(v+\frac{1}{2}\right)^2 + B_v\left[\left(J+\frac{1}{2}\right)^2 - \Lambda^2\right] - D_v J^2(J+1)^2 \pm \left[B_v^2\left(J+\frac{1}{2}\right)^2 + \frac{1}{4}\Lambda^2 A_{v,\Omega}(A_{v,\Omega} - 4B_v)\right]^{1/2}. \quad \text{(A9)}$$

The first line of this equation is the sum of the spin-orbit coupling constant $A_{v,\Omega}$ [*vide infra* Eq. (A1a)] and the vibrational energy, which contains the harmonic and anharmonic frequencies ω_e and $\omega_e x_e$, respectively. The second and third lines of Eq. (A9) give the rotational energy. [Note that the rotational energy includes the displacement due to the spin-uncoupling operator in the rotational Hamiltonian (A7b).] For a regular spin-orbit multiplet (e.g., in NO) the plus and minus signs in the rotational energy correspond to $|\Omega|=3/2$ and $1/2$, respectively. (Gallagher *et al.* [25] give a useful form of the rotational energy that is applicable if spin uncou-

pling is weak.) In the rotational energy, the rotational constants B_v and D_v, corrected to incorporate the rotation-vibration interaction in vibrational state v, are [74]

$$B_v \equiv B_e - \alpha_e\left(v + \frac{1}{2}\right), \tag{A10a}$$

$$D_v \equiv D_e + \beta_e\left(v + \frac{1}{2}\right), \tag{A10b}$$

where B_e and D_e are the equilibrium rotational and centrifugal distortion constants, and α_e and β_e are vibration-rotation interaction constants.

[1] S. Chu, Rev. Mod. Phys. **70**, 685 (1998).
[2] C. N. Cohen-Tannoudji, Rev. Mod. Phys. **70**, 707 (1998).
[3] W. D. Phillips, Rev. Mod. Phys. **70**, 721 (1998).
[4] E. A. Cornell and C. E. Wieman, Rev. Mod. Phys. **74**, 875 (2002).
[5] W. Ketterle, Rev. Mod. Phys. **74**, 1131 (2002).
[6] J. D. Weinstein, R. deCarvalho, T. Guillet, B. Friedrich, and J. M. Doyle, Nature (London) **395**, 148 (1998).
[7] H. L. Bethlem, G. Berden, F. M. N. Crompvoets, R. T. Jongma, A. J. A. V. Roij, and G. Meijer, Nature (London) **406**, 1558 (2000).
[8] J. L. Bohn, Phys. Rev. A **63**, 052714 (2001).
[9] A. V. Avdeenkov and J. L. Bohn, Phys. Rev. A **66**, 052718 (2002).
[10] P. Soldán, M. T. Cvitaš, J. M. Hutson, P. Honvault, and J. M. Launay, Phys. Rev. Lett. **89**, 153201 (2002).
[11] J. L. Bohn, A. V. Avdeenkov, and M. P. Deskevich, Phys. Rev. Lett. **89**, 203202 (2002).
[12] P. Soldán and J. M. Hutson, Phys. Rev. Lett. **92**, 163202 (2004).
[13] A. V. Avdeenkov and J. L. Bohn, Phys. Rev. Lett. **90**, 043006 (2003).
[14] A. V. Avdeenkov, D. C. E. Bortolotti, and J. L. Bohn, Phys. Rev. A **69**, 012710 (2004).
[15] D. DeMille, Phys. Rev. Lett. **88**, 067901 (2002).
[16] N. E. Shafer-Ray, K. A. Milton, B. R. Furneaux, E. R. I. Abraham, and G. R. Kalbfleisch, Phys. Rev. A **67**, 045401 (2003).
[17] D. DeMille, F. Bay, S. Bickman, D. Kawall, D. Krause, Jr., S. E. Maxwell, and L. R. Hunter, Phys. Rev. A **61**, 052507 (2000).
[18] J. J. Hudson, B. E. Sauer, M. R. Tarbutt, and E. A. Hinds, Phys. Rev. Lett. **89**, 023003 (2002).
[19] M. R. Tarbutt, H. L. Bethlem, J. J. Hudson, V. L. Ryabov, V. A. Ryzhob, B. E. Sauer, G. Meijer, and E. A. Hinds, Phys. Rev. Lett. **92**, 173002 (2004).
[20] E. Abraham, B. Bichsel, and N. Shafer-Ray, Bull. Am. Phys. Soc. **48**, 128 (2003).
[21] M. Elioff, J. Valentini, and D. Chandler, Eur. Phys. J. D **31**, 385 (2004).
[22] M. Mizushima, Phys. Rev. **109**, 1557 (1958).
[23] M. Mizushima, *The Theory of Rotating Diatomic Molecules* (Wiley, New York, 1975).
[24] C. A. Burrus and W. Gordy, Phys. Rev. **92**, 1437 (1953).
[25] J. J. Gallagher, F. D. Bedard, and C. M. Johnson, Phys. Rev. **93**, 729 (1954).
[26] J. J. Gallagher and C. M. Johnson, Phys. Rev. **103**, 1727 (1956).
[27] C. A. Burrus and J. D. Graybeal, Phys. Rev. **109**, 1553 (1958).
[28] P. G. Favero, A. M. Mirri, and W. Gordy, Phys. Rev. **114**, 1534 (1959).
[29] A. R. Hoy, J. W. C. Johns, and A. R. W. McKellar, Can. J. Phys. **53**, 2029 (1975).
[30] R. A. Frosch and H. M. Foley, Phys. Rev. **88**, 1337 (1952).
[31] M. Mizushima, Phys. Rev. **94**, 569 (1954).
[32] R. Beringer, E. B. Rawson, and A. F. Henry, Phys. Rev. **94**, 343 (1954).
[33] C. C. Lin and M. Mizushima, Phys. Rev. **100**, 1726 (1955).
[34] M. Mizushima, Phys. Rev. **105**, 1262 (1957).
[35] W. L. Meerts and A. Dymanus, J. Mol. Spectrosc. **44**, 320 (1972).
[36] P. C. Condylis, J. J. Hudson, M. R. Tarbutt, B. E. Sauer, and E. A. Hinds, J. Chem. Phys. **123**, 231101 (2005).
[37] B. Friedrich, Eur. Phys. J. D **31**, 313 (2004).
[38] J. Kalnins, G. Lambertson, and H. Gould, Rev. Sci. Instrum. **73**, 2557 (2002).
[39] H. Nishimura, G. Lambertson, J. G. Kalnins, and H. Gould, Eur. Phys. J. D **31**, 359 (2004).
[40] B. Friedrich and D. Herschbach, J. Phys. Chem. A **103**, 10280 (1999).
[41] L. Cai, J. Marango, and B. Friedrich, Phys. Rev. Lett. **86**, 775 (2001).
[42] K. K. Chakravorty, D. H. Parker, and R. B. Bernstein, Chem. Phys. **68**, 1 (1982).
[43] S. R. Gandhi, T. J. Curtiss, Q. X. Xu, S. E. Choi, and R. B. Bernstein, Chem. Phys. Lett. **132**, 6 (1986).
[44] E. R. Hudson, J. R. Bochinski, H. J. Lewandowski, B. C. Sawyer, and J. Ye, Eur. Phys. J. D **31**, 351 (2004).
[45] F. Harren, D. H. Parker, and S. Stolte, Comments At. Mol. Phys. **26**, 109 (1991).
[46] H. Ohoyama, T. Ogawa, and T. Kasai, J. Phys. Chem. **99**, 13606 (1995).
[47] T. D. Hain, M. A. Weibel, K. M. Backstrand, and T. J. Curtiss, J. Phys. Chem. A **101**, 7674 (1997).
[48] J. R. Bochinski, E. R. Hudson, H. J. Lewandowski, and J. Ye, Phys. Rev. A **70**, 043410 (2004).
[49] T. Junglen, T. Rieger, S. A. Rangwala, P. W. H. Pinkse, and G. Rempe, Eur. Phys. J. D **31**, 365 (2004).
[50] S. Y. T. van de Meerakker, P. H. M. Smeets, N. Vanhaecke, R. T. Jongma, and G. Meijer, Phys. Rev. Lett. **94**, 023004 (2005).
[51] H. L. Bethlem, G. Berden, A. J. A. van Roij, F. M. H. Crompvoets, and G. Meijer, Phys. Rev. Lett. **84**, 5744 (2000).
[52] F. M. H. Crompvoets, H. L. Bethlem, R. T. Jengmna, and G. Meijer, Nature (London) **411**, 174 (2001).
[53] J. R. Bochinski, E. R. Hudson, H. J. Lewandowski, G. Meijer, and J. Ye, Phys. Rev. Lett. **91**, 243001 (2003).
[54] M. R. Tarbutt, H. L. Bethlem, J. J. Hudson, V. L. Ryabov, V. A. Ryzhov, B. E. Sauer, G. Meijer, and E. A. Hinds, Phys. Rev. Lett. **92**, 173002 (2004).

[55] T. Rieger, T. Junglen, S. A. Rangwala, P. W. H. Pinkse, and G. Rempe, Phys. Rev. Lett. **95**, 173002 (2005).
[56] I. Roeggen, J. Phys. B **4**, 168 (1971).
[57] C. H. Townes and A. L. Schawlow, *Microwave Spectroscopy* (Dover, New York, 1975).
[58] R. Janoschek, Pure Appl. Chem. **73**, 1521 (2001).
[59] G. Herzberg, *Molecular Spectra and Molecular Structure I: Spectra of Diatomic Molecules*, 2nd ed. (Van Nostrand, New York, 1950).
[60] A. H. Saleck, G. Winnewisser, and K. M. T. Yamada, Mol. Phys. **76**, 1443 (1992).
[61] M. H. Alexander *et al.*, J. Chem. Phys. **89**, 1749 (1988).
[62] E. Klisch, S. P. Belov, R. Schieder, G. Winnewisser, and E. Herbst, Mol. Phys. **97**, 65 (1999).
[63] H. W. Kroto, *Molecular Rotation Spectra* (Wiley, New York, 1975).
[64] J. M. Brown, J. T. Hougen, K. P. Huber, J. W. C. Johns, L. Kopp, H. Lefebre-Brion, A. M. Merer, D. A. Ramsey, J. Rostas, and R. N. Zare, J. Mol. Spectrosc. **55**, 500 (1975).
[65] J. H. Van Vleck, Phys. Rev. **33**, 467 (1929).
[66] R. S. Mulliken and A. Christy, Phys. Rev. **38**, 87 (1931).
[67] R. de Vivie and S. D. Peyerimhoff, J. Chem. Phys. **90**, 3680 (1989).
[68] J. H. Van Vleck, Rev. Mod. Phys. **23**, 213 (1951).
[69] J. D. Graybeal, *Molecular Spectroscopy* (McGraw-Hill, New York, 1988).
[70] P. F. Bernath, *Spectra of Atoms and Molecules* (Oxford University Press, New York, 1995).
[71] E. Hill and J. H. V. Vleck, Phys. Rev. **32**, 250 (1928).
[72] F. H. Geuzebroek, M. G. Tenner, A. W. Kleyn, and H. Zacharias, Chem. Phys. Lett. **187**, 520 (1991).
[73] R. N. Zare, A. L. Schmeltekopf, W. J. Harrop, and D. L. Albritton, J. Mol. Spectrosc. **46**, 33 (1973).
[74] A. Goldman and S. C. Schmidt, J. Quant. Spectrosc. Radiat. Transf. **15**, 127 (1975).
[75] H. Lefebvre-Brion and R. W. Field, *Perturbations in the Spectra of Diatomic Molecules* (Academic Press, New York, 1986).
[76] K. P. Huber and G. Herzberg, *Constants of Diatomic Molecules*, Molecular Spectra and Molecular Structure IV (Van Nostrand Reinhold, New York, 1979).
[77] W. T. Rawlins, M. E. Fraser, and S. M. Miller, J. Phys. Chem. **93**, 1097 (1989).
[78] A. Amiot, J. Mol. Spectrosc. **94**, 150 (1982).
[79] A. H. Saleck, K. M. T. Yamada, and G. Winnewisser, Mol. Phys. **72**, 1135 (1991).
[80] K. J. Hallin, J. W. C. Johns, D. W. Lepart, A. W. Mantz, D. L. Wall, and K. N. Rao, J. Mol. Spectrosc. **74**, 26 (1979).
[81] H. Margenau and A. Henry, Phys. Rev. **78**, 587 (1950).
[82] C. Amiot, R. Bacis, and G. Guelachvili, Can. J. Phys. **56**, 251 (1978).
[83] A. S. Pine, J. W. C. Johns, and A. G. Robiette, J. Mol. Spectrosc. **74**, 52 (1979).
[84] R. M. Neumann, Astrophys. J. **161**, 779 (1970).
[85] F. P. Billingsley II, J. Chem. Phys. **62**, 864 (1975).
[86] S. R. Langhoff, C. W. Bauschiler, Jr., and H. Partridge, J. Chem. Phys. **89**, 4909 (1988).
[87] S. R. Langhoff, C. W. Bauschlicher, Jr., and H. Partridge, Chem. Phys. Lett. **223**, 416 (1994).
[88] W. T. Rawlins, J. C. Person, M. E. Fraser, S. M. Miller, and W. A. M. Blumberg, J. Chem. Phys. **109**, 3409 (1998).
[89] Y. Liu, Y. Guo, J. Lin, G. Huang, C. Duan, and F. Li, Mol. Phys. **99**, 1457 (2001).
[90] M. G. Tenner, E. W. Kuipers, W. Y. Langhout, A. W. Kleyn, G. Nicolasen, and S. Stolte, Surf. Sci. **236**, 151 (1990).
[91] T. Helgaker, P. Jørgensen, and J. Olsen, *Molecular Electronic-Structure Theory* (Wiley, New York, 2000).
[92] The actual basis states for this calculation should be the e/f eigenstates. Strictly, these states are perturbed by the L-uncoupling operator and so are not actually simple linear combinations of the $|\Omega\rangle$ states as in Eqs. (A6a) and (A6b). But the off-diagonal matrix elements of the L-uncoupling operator are so small compared to the splitting $\Delta\epsilon^{fe}_{v,J,\Omega}$ between the e and f states that we can neglect the first-order corrections to the perturbed e and f eigenfunctions and use the zero-field states of Eqs. (A6b) (see p. 127 of Ref. [75]).
[93] Other authors have considered the quadratic Stark effect for NO taking into account hyperfine structure [22,29]. Current experiments with cold molecules produce trapped samples at temperatures on the order of 0.1–1 K [7,117]. At these temperatures, the hyperfine splitting in NO is negligible. While introducing hyperfine interactions will be important for experiments that further cool (through evaporative or sympathetic cooling) trapped samples to energies on the size of the hyperfine splittings, this additional complexity is at present unnecessary.
[94] B. Ghaffari, J. M. Gerton, W. I. McAlexander, K. E. Strecker, D. M. Homan, and R. G. Hulet, Phys. Rev. A **60**, 3878 (1999).
[95] E. Nikitin, E. Dashevskaya, J. Alnis, M. Auzinsh, E. R. I. Abraham, B. R. Furneaux, M. Keil, C. McRaven, N. Shafer-Ray, and R. Waskowsky, Phys. Rev. A **68**, 023403 (2003).
[96] S. A. Rangwala, T. Junglen, T. Rieger, P. W. H. Pinkse, and G. Rempe, Phys. Rev. A **67**, 043406 (2003).
[97] S. Stole, J. Reuss, and H. Schwartz, Physica (Amsterdam) **57**, 254 (1972).
[98] D. V. D. Ende and S. Stolte, Chem. Phys. **89**, 121 (1984).
[99] B. Bichsel, C. McRaven, M. A. Morrison, N. Shafer-Ray, and E. R. I. Abraham (unpublished).
[100] W. G. Mallard, J. H. Miller, and K. C. Smyth, J. Chem. Phys. **76**, 3483 (1982).
[101] D. A. Dall, SIMION 3D version 7.0 (Bechtel BWXT IDAHO, LLC, 2000).
[102] We have found that two previous calculations of Stark shifts are in error. Mizushima [22] presents linear Stark shifts for the $J=1/2$, $M_J=1/2$ and $J=3/2$, $M_J=1/2,3/2$ states. We find his results to be an order of magnitude too large. In addition, Hoy *et al.* [29] presents a graph of the $J=3/2$ and $J=5/2$ rovibrational levels for these two spin-orbit states for field strengths up to 50 kV/cm based on the linear and quadratic perturbation approximations, respectively. For the $^2\Pi_{3/2}$ state, we find that their graphical result is too large by approximately a factor of 2.
[103] Diverse symbols for this quantity proliferate through the literature, including **j**, **N**, **R**, and **J**. We have chosen **N** because it is the only one of the commonly used symbols that does not represent another physical observable.
[104] The operator $\hat{\sigma}_v(xz)$ acts on electronic coordinates in the *molecular* reference frame. But the *conventional* definition of the total-parity operator, which is denoted by $\hat{E}^*$, is the operator that inverts electronic (and nuclear) coordinates *in a space-fixed ("laboratory") coordinate system*. Hougen [108]

showed that the effect of $\hat{\sigma}_v(xz)$ on a rovibronic wave function in the molecular frame is equivalent to the action of $\hat{E}^*$ in the laboratory frame. Because electronic wave functions are calculated in the molecular frame, discussions of the parity of molecular wave functions are couched in terms of $\hat{\sigma}_v(xz)$ rather than $\hat{E}^*$.

[105] In earlier literature on Λ doubling (see, for example, Refs. [65,66]), these states were denoted c and d. In this notation, the $|d\rangle$ state of a particular rotational (J) state of a particular spin-orbit electronic state of NO lies above the $|c\rangle$ state. The symmetry properties of these states have been analyzed by Alexander and Dagdigian [112] and an alternative proposed notation in Alexander *et al.* [61]. In their notation, the Λ-doublet states of the $^2\Pi_{1/2}$ level are denoted $\Pi(A')$ and $\Pi(A'')$, respectively; these designations are reversed for the $^2\Pi_{3/2}$ level.

[106] Note that electric dipole transitions in NO are governed by the selection rules $e \leftrightarrow f$ for the Q branch and $e \leftrightarrow e$ and $f \leftrightarrow f$ for the P and R branches.

[107] S. Green and R. N. Zare, Chem. Phys. **7**, 62 (1975).

[108] J. T. Hougen, Technical Report No. 115, Nat. Bur. Stand., Washington, D.C., 1970 (unpublished).

[109] See, Eur. Phys. J. D **31** (2004), special issue on cold polar molecules.

[110] In some contexts, the suitability of a perturbative treatment of this effect is not an issue. For example, applications of the Stark effect to Rydberg states of atoms and molecules [113,114] cannot be analyzed using perturbation theory—or, for that matter, using a few-state model. In addition, perturbation theory is sometimes inappropriate for analysis of electrostatic manipulation and trapping of polyatomic molecules, due to the large number of closely spaced quantum states [115,116].

[111] R. N. Dixon and D. Field, Proc. R. Soc. London, Ser. A **368**, 99 (1979).

[112] M. H. Alexander and P. D. Dagdigian, J. Chem. Phys. **80**, 4325 (1984).

[113] Y. Yamakita, S. R. Procter, A. L. Goodgame, T. P. Softley, and F. Merkt, J. Chem. Phys. **121**, 1419 (2004).

[114] M. J. J. Vrakking, J. Chem. Phys. **105**, 7336 (1996).

[115] S. A. Rangwala, T. Junglen, T. Rieger, P. W. H. Pinkse, and G. Rempe, Phys. Rev. A **67**, 043406 (2003).

[116] J. V. Veldhoven, J. Küpper, H. L. Bethlem, B. Sartakov, A. J. A. V. Roij, and G. Meijer, Eur. Phys. J. D **31**, 337 (2004).

[117] H. L. Bethlem and G. Meijer, Int. Rev. Phys. Chem. **22**, 73 (2003).